

# Overview of experimental critical point search

Tobiasz Czopowicz<sup>1,2</sup>

<sup>1</sup> Jan Kochanowski University, Kielce, Poland

<sup>2</sup> Warsaw University of Technology, Warsaw, Poland  
Tobiasz.Czopowicz@cern.ch

**Abstract.** The existence and location of the QCD critical point is an object of vivid experimental and theoretical studies. Rich and beautiful data recorded by experiments at SPS and RHIC allow for a systematic search for the critical point – the search for a non-monotonic dependence of various correlation and fluctuation observables on collision energy and size of colliding nuclei.

**Keywords:** Quark-Gluon Plasma, critical point, fluctuations

## 1 Critical point search strategies

A sketch of the most popular phase diagram of strongly-interacting matter is shown in Fig. 1. At low temperatures and baryon chemical potential, the system consists of quarks and gluons confined inside hadrons. At higher temperature and/or baryon chemical potential, quarks and gluons may act like quasi-free particles, forming a different state of matter – the Quark-Gluon Plasma. Between the two phases, a first-order transition is expected at high  $\mu$ . Critical point (CP) is a hypothetical end point of this first-order phase transition line that has properties of a second-order phase transition [1,2].

It is commonly expected that the QCD critical point should lead to an anomaly in fluctuations in a narrow domain of the phase diagram. However predictions on the CP existence, its location and what and how should fluctuate are model dependent [3].

The experimental search for the critical point requires a two-dimensional scan in freeze-out parameters ( $T$ ,  $\mu$ ) by changing collision parameters controlled in laboratory, i.e. energy and size of the colliding nuclei (or collision centrality).

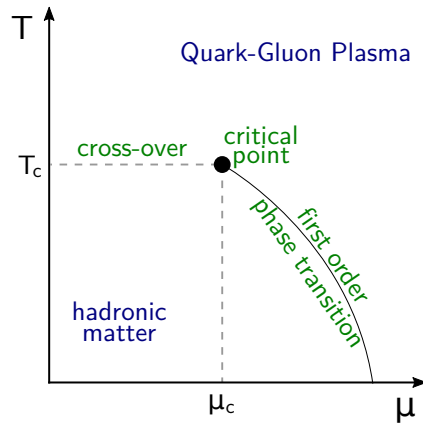


**Fig. 1.** A sketch of the phase diagram of strongly-interacting matter.

## 2 Experimental measures

### 2.1 Extensive quantities

An extensive quantity is a quantity that is proportional to the number of Wounded Nucleons (W) in the Wounded Nucleon Model [4] (WNM) or to the volume (V) in the Ideal Boltzmann Grand Canonical Ensemble (IB-GCE). The most popular are particle number (multiplicity) distribution  $P(N)$  cumulants:

$$\begin{aligned}\kappa_1 &= \langle N \rangle, \\ \kappa_2 &= \langle (\delta N)^2 \rangle = \sigma^2, \\ \kappa_3 &= \langle (\delta N)^3 \rangle = S\sigma^3, \\ \kappa_4 &= \langle (\delta N)^4 \rangle - 3\langle (\delta N)^2 \rangle^2 = \kappa\sigma^4.\end{aligned}$$

### 2.2 Intensive quantities

Ratio of any two extensive quantities is independent of W (WNM) or V (IB-GCE) for an event sample with fixed W (or V) – it is an intensive quantity. For example:

$$\langle A \rangle / \langle B \rangle = W \cdot \langle a \rangle / W \cdot \langle b \rangle = \langle a \rangle / \langle b \rangle,$$

where  $A$  and  $B$  are any extensive event quantities, i.e.  $\langle A \rangle \sim W$ ,  $\langle B \rangle \sim W$  and  $\langle a \rangle = \langle A \rangle$  and  $\langle b \rangle = \langle B \rangle$  for  $W = 1$ . Popular examples are:

$$\begin{aligned}\kappa_2/\kappa_1 &= \omega[N] = \frac{\sigma^2[N]}{\langle N \rangle} = \frac{W \cdot \sigma^2[n]}{W \cdot \langle n \rangle} = \omega[n] \text{ (scaled variance)}, \\ \kappa_3/\kappa_2 &= S\sigma, \\ \kappa_4/\kappa_2 &= \kappa\sigma^2.\end{aligned}$$

### 2.3 Strongly intensive quantities

For an event sample with varying W (or V), cumulants are not extensive quantities any more. For example:

$$\kappa_2 = \sigma^2[N] = \sigma^2[n] \langle W \rangle + \langle n \rangle^2 \sigma^2[W].$$

However, having two extensive event quantities, one can construct quantities that are independent of the fluctuations of W (or V). Popular examples include [5,6]:

$$\begin{aligned}\langle K \rangle / \langle \pi \rangle, \\ \Delta[N, P_T] &= (\omega[N] \langle P_T \rangle - \omega[P_T] \langle N \rangle) / c, \\ \Sigma[N, P_T] &= (\omega[N] \langle P_T \rangle + \omega[P_T] \langle N \rangle - 2(\langle NP_T \rangle - \langle P_T \rangle \langle N \rangle)) / c,\end{aligned}$$

where  $P_T = \sum_{i=1}^N p_{T,i}$  and  $C$  is any extensive quantity (e.g.  $\langle N \rangle$ ).

### 2.4 Short-range correlations

Quantum statistics leads to short-range correlations in momentum space, which are sensitive to particle correlations in configuration space (e.g. of CP origin).

Popular measures include momentum difference in Longitudinal Comoving System (LCMS),  $\mathbf{q}$ , that is decomposed into three components:  $q_{long}$  – denoting momentum difference along the beam,  $q_{out}$  – parallel to the pair transverse-momentum vector ( $\mathbf{k}_t = (\mathbf{p}_{T,1} + \mathbf{p}_{T,2})/2$ ) and  $q_{side}$  – perpendicular to  $q_{out}$  and  $q_{long}$ . The two-particle correlation function  $C(q)$  is often approximated by a three-dimensional Gauss function:

$$C(\mathbf{q}) \cong 1 + \lambda \cdot \exp\left(-R_{long}^2 q_{long}^2 - R_{out}^2 q_{out}^2 - R_{side}^2 q_{side}^2\right),$$

where  $\lambda$  describes the correlation strength and  $R_{out}, R_{side}, R_{long}$  denote Gaussian HBT radii.

A more parametrization of the correlation function is possible via introducing Lévy-shaped source (1-D) [7]:

$$C(q) \cong 1 + \lambda \cdot e^{(-qR)^\alpha},$$

where  $q = |p_1 - p_2|_{LCMS}$ ,  $\lambda$  describes correlation length,  $R$  determines the length of homogeneity and Lévy exponent  $\alpha$  determines source shape:  $\alpha = 2$ : Gaussian, predicted from a simple hydro,  $\alpha < 2$ : anomalous diffusion, generalized central limit theorem,  $\alpha = 0.5$ : conjectured value at the critical point.

## 2.5 Fluctuations as a function of momentum bin size

When a system crosses the second-order phase transition, it becomes scale invariant, which leads to power-law form of correlation function. The second factorial moment is calculated as a function of the momentum cell size (or bin number  $M$ ):

$$F_2(M) \equiv \left\langle \frac{1}{M} \sum_{i=1}^M n_i(n_i - 1) \right\rangle \bigg/ \left\langle \frac{1}{M} \sum_{i=1}^M n_i \right\rangle,$$

where  $n_i$  is particle multiplicity in cell  $i$ .

At the second-order phase transition the system is a simple fractal and the factorial moment exhibits a power-law dependence on  $M$  [8,9,10,11]:

$$F_2(M) \sim (M)^{\varphi_2}.$$

In case the system freezes-out in the vicinity of the critical point,  $\varphi_2 = 5/6$ .

To cancel the  $F_2(M)$  dependence on the single-particle inclusive momentum distribution, one needs a uniform distribution of particles in bins or subtraction of the  $F_2(M)$  values for mixed events:

$$\Delta F_2(M) = F_2^{data}(M) - F_2^{mixed}(M).$$

## 2.6 Light nuclei production

Based on coalescence model, particle ratios of light nuclei are sensitive to the nucleon density fluctuations at kinetic freeze-out and thus to CP. In the vicinity of the critical point or the first-order phase transition, density fluctuation becomes larger [12,13].

Nucleon density fluctuation can be expressed by proton, triton and deuteron yields as:

$$\Delta n = \frac{\langle (\delta n)^2 \rangle}{\langle n \rangle} \approx \frac{1}{2\sqrt{3}} \frac{N_p \cdot N_t}{N_d^2} - 1.$$

### 3 Experimental results

#### 3.1 Multiplicity fluctuations

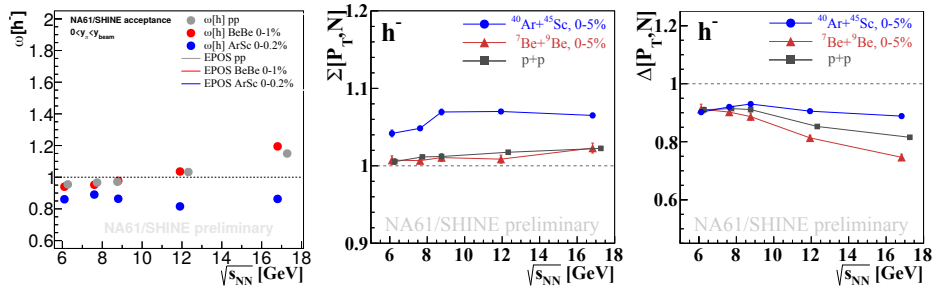


**Fig. 2.** Results on multiplicity [14] (*left*) and multiplicity-transverse momentum [15] (*center, right*) fluctuations for all negatively charged particles recorded by NA61/SHINE.

Results on energy dependence of multiplicity fluctuations by NA61/SHINE [14] quantified by the scaled variance are presented in Fig. 2 (*left*). No prominent structures that could be related to the critical point are observed.

#### 3.2 Multiplicity-transverse momentum fluctuations

Results on energy dependence of multiplicity-transverse momentum fluctuations by NA61/SHINE [15] expressed in  $\Delta$  and  $\Sigma$  strongly intensive quantities are presented in Fig. 2 (*center, right*). No prominent structures that could be attributed to the critical point are observed.

#### 3.3 Net-proton fluctuations

Figure 3 (*left*) presents energy dependence of fourth-order net-proton fluctuation in 5% most central Au+Au collisions recorded by STAR [16]. The observed non-monotonic dependence is consistent with theoretical predictions [17] and might suggest a critical point around  $\sqrt{s_{NN}} \approx 7$  GeV.

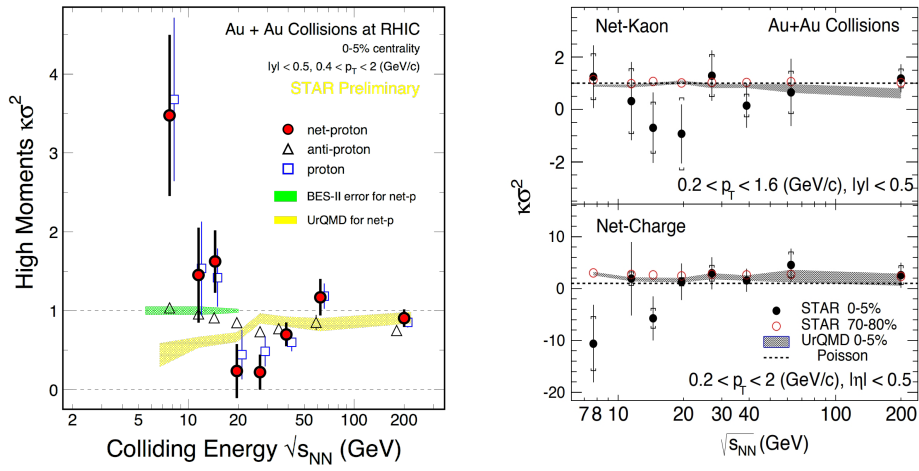


**Fig. 3.** Results on  $\kappa\sigma^2$  of net-proton [16] (left) as well as net-kaon and net-charge [18,19] (right) distributions measured by STAR.

### 3.4 Net-kaon and net-charge fluctuations

The STAR Collaboration has also studied net-kaon and net-charge distributions in central Au+Au collisions [18,19]. However, the results, presented in Fig. 3 (right), show no (within errors) energy dependence.

### 3.5 Short-range correlations

**Finite-Size Scaling** Fig. 4 presents compilations of Au+Au ( $\sqrt{s_{NN}} = 7.7\text{--}200$  GeV) data from STAR [21] and Pb+Pb ( $\sqrt{s_{NN}} = 2.76$  TeV) data from ALICE [22]. The Gaussian emission source radii ( $R_{out}^2 - R_{side}^2$ ) [20] show clear non-monotonic energy dependence with a maximum at  $\sqrt{s_{NN}} \approx 47.5$  GeV. The initial Finite-Size Scaling analysis [20] suggests the critical point position:  $T = 165$  MeV and  $\mu = 95$  MeV.

**Transverse-mass dependence of Lévy exponent** Transverse-mass dependence of Lévy exponent  $\alpha$  have been studied both at SPS and RHIC. Figure 5 presents the results for Be+Be at 17 GeV by NA61/SHINE [23] and for Au+Au at 200 GeV by PHENIX [24]. Both studies revealed similar results, i.e.  $\alpha \approx 1.2$ , a value significantly above the CP prediction.

### 3.6 Fluctuations as a function of momentum bin size

NA49 and NA61/SHINE have studied the second factorial moment,  $\Delta F_2$ , for mid-rapidity protons at 17 GeV.

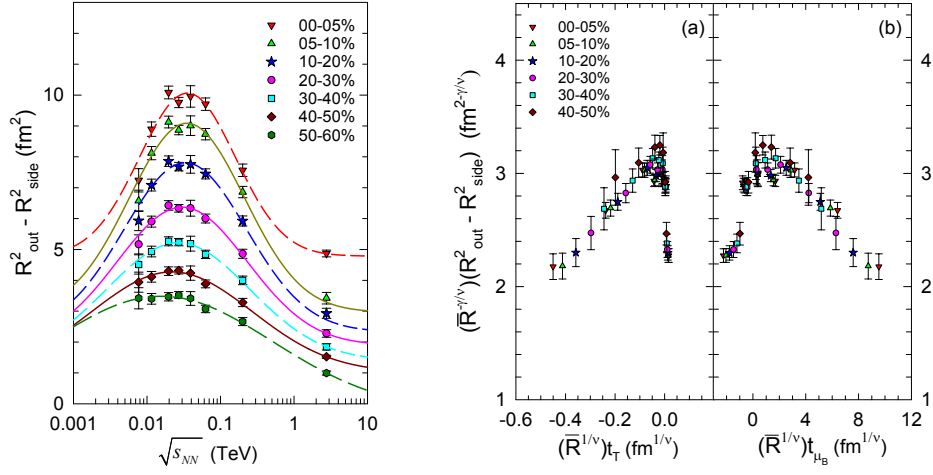


**Fig. 4.** Compilations of Au+Au ( $\sqrt{s_{NN}} = 7.7\text{--}200$  GeV, STAR [21]) and Pb+Pb ( $\sqrt{s_{NN}} = 2.76$  TeV, ALICE [22]) data: energy dependence of Gaussian emission source radii [20] (*left*) and one of the result for initial Finite-Size Scaling analysis [20] (*right*).

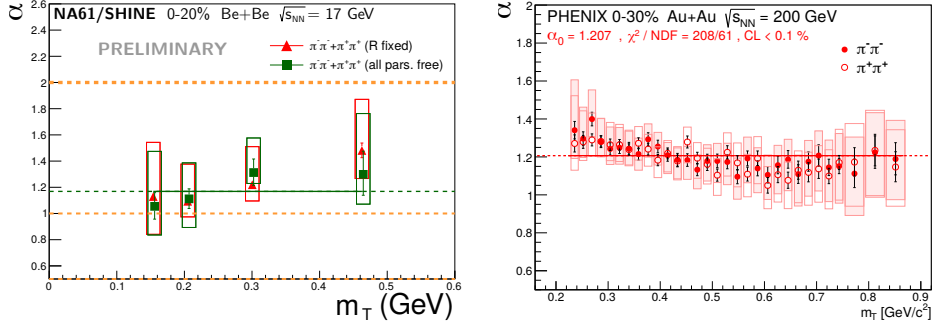


**Fig. 5.** Transverse mass dependence of the Lévy exponent  $\alpha$  for 20% most central Be+Be collisions at 17 GeV by NA61/SHINE [23] (*left*) and for 30% Au+Au at 200 GeV by PHENIX [24] (*right*).

Although in central Be+Be, C+C, Ar+Sc and Pb+Pb no signal has been observed, a deviation of  $\Delta F_2$  from zero seems apparent in central Si+Si and mid-central Ar+Sc as shown in Fig. 6.

### 3.7 Light nuclei production

The nucleon density fluctuations,  $\Delta n$ , for central Pb+Pb by NA49 [28] and central Au+Au by STAR [29,30] show a non-monotonic dependence on collision energy with a peak for  $\sqrt{s_{NN}} \approx 20$  GeV [31] as presented in Fig. 7.

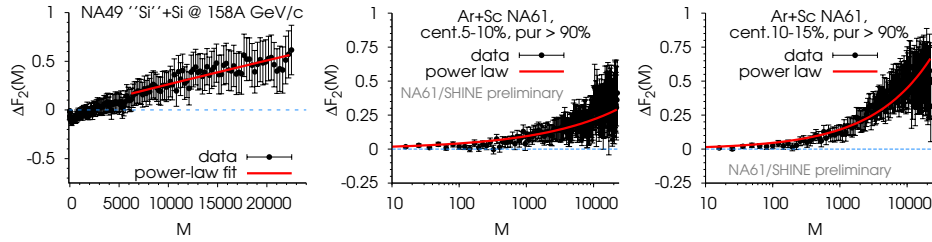


**Fig. 6.** Second factorial moment,  $\Delta F_2$ , for mid-rapidity protons at 17 GeV in Si+Si by NA49 [26] (*left*) and in 5–10% and 10–15% Ar+Sc by NA61/SINE [27] (*center, right*).

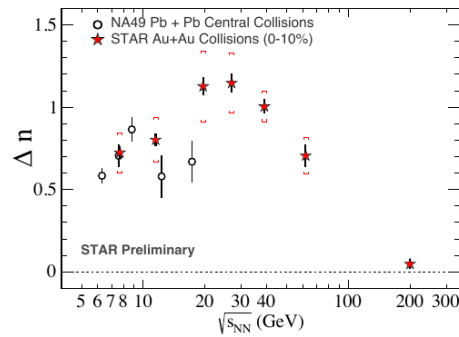


**Fig. 7.** Nucleon density fluctuation,  $\Delta n$ , for central Pb+Pb [28] and Au+Au [29,30] collisions.

## 4 Summary

The experimental search for the critical point is ongoing. There are four indications of anomalies in fluctuations in heavy-ion collisions at different collision energies ( $\sqrt{s_{NN}} \approx 7, 17, 20, 47$  GeV). Interpreting them as due to CP allows one to estimate four hypothetical CP locations depicted in Fig. 8.

Fortunately, there are high-quality, beautiful new data coming soon both from SPS (NA61/SHINE) and RHIC (STAR Beam energy Scan II).

## References

1. M. Asakawa and K. Yazaki, Nucl. Phys. A **504**, 668 (1989).
2. A. Barducci, R. Casalbuoni, S. De Curtis, R. Gatto and G. Pettini, Phys. Lett. B **231**, 463 (1989).
3. M. A. Stephanov, PoS LAT **2006**, 024 (2006).
4. A. Bialas, M. Bleszynski and W. Czyz, Nucl. Phys. B **111**, 461 (1976).
5. M. I. Gorenstein and M. Gazdzicki, Phys. Rev. C **84**, 014904 (2011).
6. M. Gazdzicki, M. I. Gorenstein and M. Mackowiak-Pawlowska, Phys. Rev. C **88**, no. 2, 024907 (2013).

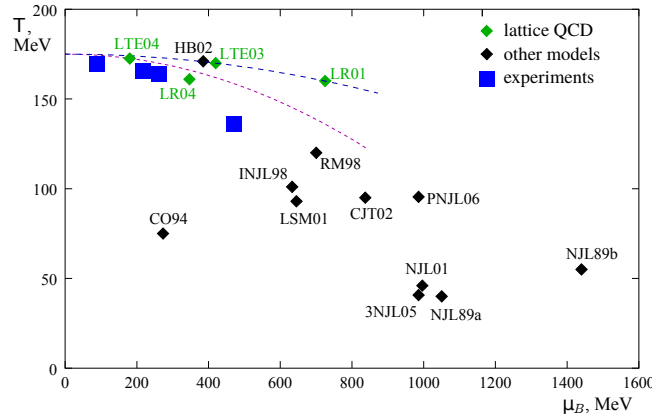


**Fig. 8.** Compilation of theoretical predictions [3] and experimental hints on the critical point location.

7. T. Csorgo, S. Hegyi, T. Novak and W. A. Zajc, AIP Conf. Proc. **828**, no. 1, 525 (2006).
8. J. Wosiek, Acta Phys. Polon. **B19**, 863 (1988).
9. A. Bialas and R. C. Hwa, Phys. Lett. B **253**, 436 (1991).
10. A. Bialas and R. B. Peschanski, Nucl. Phys. B **273**, 703 (1986).
11. N. G. Antoniou, F. K. Diakonov, A. S. Kapoyannis and K. S. Kousouris, Phys. Rev. Lett. **97**, 032002 (2006).
12. K. J. Sun, L. W. Chen, C. M. Ko and Z. Xu, Phys. Lett. B **774**, 103 (2017).
13. E. Shuryak and J. Torres-Rincon, Nucl. Phys. A **982**, 831 (2019).
14. M. Gazdzicki [NA61/SHINE Collaboration], PoS CPOD **2017**, 012 (2018).
15. E. Andronov [NA61/SHINE Collaboration], Acta Phys. Polon. Supp. **10** 449 (2017).
16. L. Adamczyk *et al.* [STAR Collaboration], Phys. Rev. Lett. **112**, 032302 (2014).
17. M. A. Stephanov, Phys. Rev. Lett. **107**, 052301 (2011).
18. L. Adamczyk *et al.* [STAR Collaboration], Phys. Lett. B **785**, 551 (2018).
19. L. Adamczyk *et al.* [STAR Collaboration], Phys. Rev. Lett. **113**, 092301 (2014).
20. R. A. Lacey, Phys. Rev. Lett. **114**, no. 14, 142301 (2015).
21. L. Adamczyk *et al.* [STAR Collaboration], Phys. Rev. C **92**, no. 1, 014904 (2015).
22. K. Aamodt *et al.* [ALICE Collaboration], Phys. Lett. B **696**, 328 (2011).
23. B. Porfy [NA61/SHINE Collaboration], Acta Phys. Polon. Supp. **12** 451 (2019).
24. A. Adare *et al.* [PHENIX Collaboration], Phys. Rev. C **97**, no. 6, 064911 (2018).
25. N. Davis *et al.* [NA61/SHINE Collaboration], PoS CPOD **2017**, 054 (2018).
26. T. Anticic *et al.* [NA49 Collaboration], Eur. Phys. J. C **75**, no. 12, 587 (2015).
27. N. Davis *et al.* [NA61/SHINE Collaboration], PoS CPOD **2017**, 054 (2018).
28. T. Anticic *et al.* [NA49 Collaboration], Phys. Rev. C **94**, no. 4, 044906 (2016).
29. L. Adamczyk *et al.* [STAR Collaboration], Phys. Rev. Lett. **121**, no. 3, 032301 (2018).
30. N. Yu [STAR Collaboration], Nucl. Phys. A **967**, 788 (2017).
31. D. Zhang [STAR Collaboration], <https://indico.cern.ch/event/656452/contributions/2859773/>.